SolarPACES 2013

A comparison of supercritical carbon dioxide power cycle configurations with an emphasis on CSP applications

T. Neises*, C. Turchi

NREL, 15013 Denver West Parkway, Golden, CO 80401, USA

Abstract

Recent research suggests that an emerging power cycle technology using supercritical carbon dioxide (s-CO2) operated in a closed-loop Brayton cycle offers the potential of equivalent or higher cycle efficiency versus supercritical or superheated steam cycles at temperatures relevant for CSP applications. Preliminary design-point modeling suggests that s-CO2 cycle configurations can be devised that have similar overall efficiency but different temperature and/or pressure characteristics. This paper employs a more detailed heat exchanger model than previous work to compare the recompression and partial cooling cycles, two cycles with high design-point efficiencies, and illustrates the potential advantages of the latter. Integration of the cycles into CSP systems is studied, with a focus on sensible heat thermal storage and direct s-CO2 receivers. Results show the partial cooling cycle may offer a larger temperature difference across the primary heat exchanger, thereby potentially reducing heat exchanger cost and improving CSP receiver efficiency.

1. Introduction

Closed-loop supercritical CO2 (s-CO2) cycles are currently being researched for application in fossil, nuclear and concentrating solar power (CSP) plants, as well in waste heat recovery and marine systems. These cycles take advantage of high density near the critical point to minimize compressor work and yield potentially higher cycle efficiency compared to superheated or supercritical steam cycles at temperatures planned for fossil, nuclear, and CSP. Additionally, these cycles are projected to have a smaller weight and volume, lower thermal mass, and less

---

* Corresponding author. Tel.: 1-303-275-4537; fax: 1-303-384-7495
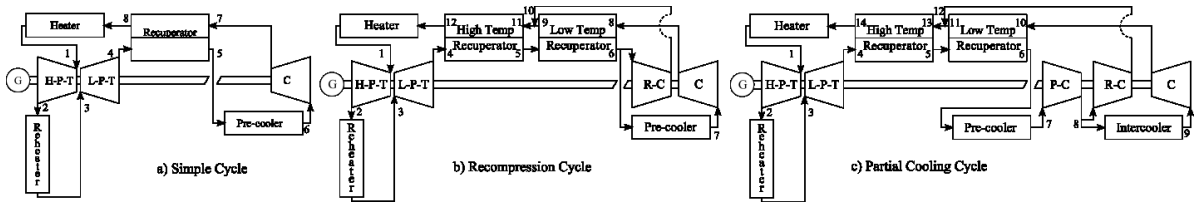 *E-mail address:* ty.neises@nrel.gov

Figure 1: Closed-loop supercritical carbon dioxide Brayton cycles studied in this paper.

complex power block than Rankine cycles. The realization of these projections may also result in reduced installation, maintenance and operation cost of the system.

Another feature of s-CO2 cycles is that multiple configurations of turbomachinery and heat exchanges can be constructed to achieve similar overall efficiency but different temperature and/or pressure characteristics that may benefit a particular cycle application. The three configurations studied in this paper are shown in Figure 1, and have been thoroughly described in the literature [1], [2].

The following two factors are the most important for integrating s-CO2 power cycles into CSP plants: 1) superior performance vs. the steam Rankine cycle at dry cooling conditions, and 2) the ability to economically integrate thermal energy storage. Due to its single phase operation, especially at the primary heat exchanger, s-CO2 matches well with sensible heat storage. Because the volume of sensible heat storage required for a given storage capacity is proportional to the temperature difference between the hot and cold heat transfer fluid (HTF) temperatures, power cycles that enable larger temperature differences are advantageous for CSP applications with sensible thermal energy storage. It is true that for a given cycle configuration the temperature difference in the cycle can be increased at the expense of the cycle efficiency, creating a very complex optimization problem. This paper instead focuses on exploring the thermal efficiency and temperature differences endemic to different cycle configurations.

1.1. Previous modeling studies

Dostal et al. [2] performed a detailed design-point study of the simple and recompression configurations for nuclear applications. The recuperator(s) and pre-cooler were modeled using a first principles model of printed circuit heat exchangers (PCHE), and the performance results of different dimensions were analyzed. The pre-cooler used cooling water as the other fluid (i.e., a wet-cooled design). The results optimized both configurations for integration with a nuclear plant and showed that one stage of reheat provided around 1.2% efficiency improvement.

Dostal and Kulhanek [3] compared the design-point performance of different cycle configurations for a wet-cooled plant at 550°C using a heat exchanger effectiveness approach to model the recuperator(s). The paper concluded that other "complex" cycle designs reached similar efficiencies as the recompression.

Seidel [4] performed a design-point study of the simple configuration using a first principles model of the PCHE used as the recuperator. This work analyzed dry, wet, and hybrid cooled plants and showed that for dry cooled plants the optimum design point increased the lower pressure well above the critical pressure in order to accommodate heat rejection at higher temperatures.

Bryant et al. [5] performed a design-point performance comparison of the simple and recompression cycles, using both effectiveness and conductance (UA) recuperator models. This analysis showed that below a certain quantity of conductance the simple cycle is as efficient as the recompression cycle.

Kulhanek and Dostal [6] studied the design-point performance of different configurations for wet-cooled cycles using an effectiveness model for the recuperator(s). They showed that the partial cooling cycle offers the largest

temperature difference across the primary heat exchanger and a higher specific work across the turbine while maintaining competitive efficiencies with the recompression cycle at relevant turbine inlet temperatures.

Previous work by NREL [1] studied the design-point performance of different configurations for dry-cooled cycles using an effectiveness model for the recuperator(s) and showed that both the partial cooling and recompression cycles with single-stage reheat have the potential to achieve the 50% thermal-to-electric efficiency target set by the U.S. DOE SunShot program.

Dyreby et al. [7] researched the design and off-design performance of the simple and recompression cycles for dry-cooled cycles using the conductance approach to model heat exchangers. Off-design performance maps of the compressor and turbine were investigated, while the conductance model solved for off-design conductance as a function of off-design and design-point mass flow rates. Dyreby has noted [8] similarly to Bryant [5], that for small allocations of recuperator conductance the simple cycle is as efficient as the recompression cycle.

While the simple configuration is the least efficient, it is often studied because it is projected as the best candidate for entry to the commercial market due to its simplicity [9]. For applications requiring high thermal efficiencies, the recompression cycle is usually selected because it reaches the highest design-point efficiencies (with the partial cooling cycle) and has the simplest cycle design; however, the reviewed comparisons between the recompression and partial cooling cycles were derived using an effectiveness model for the heat exchangers. The literature reviewed here suggests that while modeling the heat exchanger using the effectiveness approach is a good first approximation of a cycle's performance bounds, a more detailed heat exchanger model that estimates the conductance of the heat exchangers is required to make more accurate comparisons between cycle configurations.

This paper first optimizes a design case for the three selected configurations (simple, recompression, and partial cooling) using an effectiveness heat exchanger model. The required recuperator conductance is calculated and shown to vary significantly between cycle configurations applying the same recuperator effectiveness. Then, the models are solved over a range of conductance values to generate a more accurate comparison of cycle performance under equivalent heat exchanger sizing. Next, model assumptions and limitations are discussed. Finally, integration with CSP systems addressed.

Nomenclature

f_{HTR}	Fraction of total conductance allocated to the high temperature recuperator
LTR	Low temperature recuperator
HTR	High temperature recuperator
PHX	Primary heat exchanger
UA	Heat exchanger conductance

---

2. Modeling approach

The following analysis evaluates the simple, recompression, and partial cooling models shown in Figure 1. The cycle components included in the design point models are compressors, turbines, recuperators and pre-coolers. Both the compressor and turbine component models use a simple isentropic efficiency model.

The counter-flow recuperator heat exchanger modeling approach depends on whether an effectiveness or conductance is specified to characterize the recuperator. Both models discretize the heat exchanger to account for changing physical properties and solve for the conditions that result in the specified effectiveness or conductance [10]. The effectiveness model also enforces a minimum temperature difference in the recuperator that is designed to constrain the performance of the recuperator by imposing "realistic" physical bounds (although quantifying the exact impact of this constraint is difficult without using the more detailed conductance model). Validation of the

effectiveness model is shown in the previous work [10]. The conductance model uses the standard counter-flow effectiveness-NTU relationship at each discretization to calculate the total heat exchanger conductance. Note that the conductance model is sensitive to the power rating of the cycle while the effectiveness model is not.

Finally, the air-cooled finned-tube pre-cooler model used in this study was developed as a thesis project by Gavic [11]. This model is publically available, and only cosmetic changes were made to the model to allow it to be called by the cycle models – all of the performance calculations are unchanged from the published version.

These components were coded as subprograms or procedures in Engineering Equation Solver (EES) [12]. The cycle model solves by calling these subprograms/procedure as necessary and applying the following assumptions and constraints:

- The turbine inlet temperature is set as a constant value. This value is not optimized as it is known that increasing it will increase cycle efficiency. The model assumes that a primary heat exchanger exists that can meet the required thermal input and turbine inlet temperature.
- The compressor inlet temperature is set as a constant value. In a more detailed design study, this value may be optimized along with pre-cooler size and cooling fan parasitic. This study calculates the pre-cooler size required to meet the selected compressor inlet temperature as a function of ambient conditions, inlet conditions, load, and fraction of new power output allocated for fan parasitics.
- In the recompression and partial cooling cycles, the model is constrained such that the compressor outlet temperature of the flow that bypasses the low temperature recuperator is set equal to the high pressure outlet temperature of the recuperator (i.e., the temperatures at points 9, 10, and 11 are equal in Figure 1a, and the temperatures 11, 12, and 13 are equal in Figure 1b). This approach is consistent with the literature.
- This study neglects pressure drops in the heat exchangers.
- One stage of reheat is modeled for each configuration. The intermediate pressure is set as the average of the high and low side pressures [2].
- Heat exchanger performance is defined by specifying a performance metric, which depends on the heat exchanger model used. In the recompression and partial cooling cycles using the effectiveness approach, the high temperature recuperator and overall hot side effectiveness are specified, which matches Dostal's approach [6]. When the conductance model is applied, the combined recuperator conductance and the fraction of conductance allotted to the high temperature recuperator are specified. It is clear that increasing the combined conductance will improve cycle efficiency (at least for the current case ignoring pressure drops). However, it is not intuitive how the combined recuperator conductance should be allocated between the high and low temperature recuperators for the recompression and partial cooling cycles. Therefore, the fraction allocated to the high temperature recuperator is optimized for each design case.
- The upper pressure is set to a constant value. The pressure ratio, which defines the lower pressure, is optimized for each design case.
- The partial cooling cycle requires an intermediate compressor pressure. This value is defined by the ratio of pressure ratios (*rpr*), Equation 1, and is also optimized for each design case.
- All optimization was completed using the "Variable Metric" method built into EES.

$$rpr = \frac{\dfrac{P_{high}}{P_{intermediate}} - 1}{\dfrac{P_{high}}{P_{low}} - 1} \qquad (1)$$

3. Design values

Table 1 shows the values of the design parameters used in this study, along with brief comments explaining their selection, while Table 2 shows the values of design parameters required for the air-cooled, finned-tube, pre-cooler

model. The values in these tables fully constrain the model and allow for the modeling results presented in the next section to be reproduced.

Table 1: Design and optimized parameters for cycle case studies

Design Parameters	Value	Comments
Turbine efficiency	93%	Projection of mature, commercial size axial flow turbine efficiency
Compressor efficiency	89%	Projection of mature, commercial size radial compressor
Heat exchanger effectiveness	97%	5°C minimum temperature difference, neglect pressure drops
Heat exchanger conductance (UA)	Varied MW/K	Neglect pressure drops
Turbine inlet temperature	650°C	SunShot target for CSP power tower outlet temperatures
Compressor inlet temperature	50°C	Possible under dry cooling with 15°C ITD, 35°C ambient temperature
Upper pressure	25 MPa	Upper limit given available and economic piping
Turbine Stages	2	One stage of reheat at average of high and low side pressures
Net power output	35 MW	Estimate of power cycle requirements for a 100 MW-thermal SunShot target power tower with a solar multiple of 1.5
Optimized Parameters	**Relevant Cycles**	
Pressure ratio (PR)	All	
f_{HTR}	Recompression, Partial Cooling (not applicable for effectiveness approach)	
Ratio of pressure ratios (rpr)	Partial Cooling	

Table 2: Design parameters to calculate the air-cooled, finned-tube, pre-cooler mass given cycle state points

Design Parameters	Value	Comments
Configuration	fc_tubes_s80-38T	Shown by Gavic to have low material usage [11]
Number of loops	3	Number of passes s-CO2 makes across air flow
Number of nodes	10	Number of nodes used to discretize one pass of s-CO2
Material	Stainless AISI302	Common low temperature material
Tube thickness	0.5 mm	Reasonable value for observed pressure and temperatures
Cooling fan power	0.35 MW	Limit to 1% of net power output to estimate a possible design
Ambient Pressure	1 atm	Ambient pressure at sea level

4. Results

First, the effectiveness/minimum-temperature approach is optimized for each configuration using the design conditions in Table 1, and the required recuperator conductance is calculated. The results in Table 3 show that for the selected design conditions, the recompression cycle conductance is almost twice as large as the partial cooling cycle conductance, while achieving an only slightly improved thermal efficiency. However, the mass of the pre-cooler is around 22% larger in the partial cooling cycle than in the recompression cycle. The simple cycle has the lowest conductance, but suffers a 5% efficiency penalty.

Table 3: Optimized modeling results using effectiveness model and design effectiveness to model recuperator

Cycle	PR	rpr	*Efficiency	Split Fraction	UA LTR	UA HTR	UA Combined	Pre-cooler Mass
	-	-	%	-	MW/K	MW/K	MW/K	ton
Simple	3.4	-	44.60	-	-	3.04	3.04	61.6
Recompression	2.5	-	49.66	0.71	3.21	5.33	8.54	49.7
Partial Cooling	4.55	0.369	49.53	0.59	1.73	2.60	4.33	63.8

*Note that the reported thermal efficiency does not include fan parasitics, which are 0.35 MW for each case.
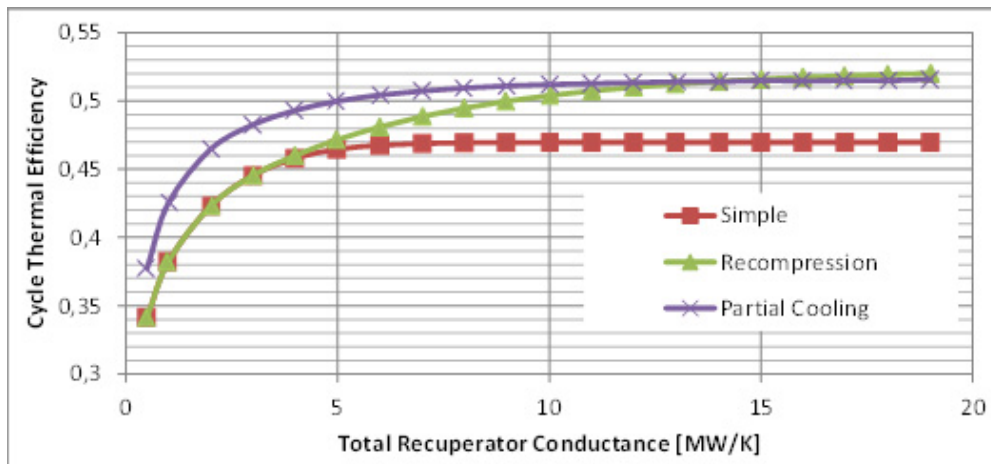

Figure 2: Optimized cycle thermal efficiency versus total recuperator conductance

Because of the large difference in calculated conductance when the recuperator effectiveness/minimum-temperature model is used, it is difficult to compare the cycle performance on an equivalent basis. To better understand the relationship between cycle performance and conductance, each cycle configuration was solved using the conductance model for the recuperator over a range of values. Figure 2 shows that when the cycles are compared with equal conductance values, the partial cooling cycle asymptotes towards its highest efficiency at much lower conductance values than the recompression cycle. Additionally, this analysis shows the overlap at low conductance values between the simple and recompression cycles that has been observed by others [5], [8].

If it can be assumed that cycle cost is largely driven by the required recuperator conductance, then the partial cooling cycle appears advantageous at these design conditions up to about 15 MW/K of conductance. Table 4 shows additional relevant cycle metrics at three different conductance levels. It is also notable that the high temperature recuperator in the partial cooling cycle experiences a maximum temperature around 50°C lower than the recompression cycle, which may help reduce its relative cost. At each level, the recompression maintains its advantage in pre-cooler mass. This may be due to the fact the recompression rejects all of its heat at higher pressures, which provides a more favorable temperature profile for heat rejection [4].

Table 4: Optimized modeling results using conductance model to model recuperator at various levels of conductance

Cycle	Recup UA	f_{HTR}	P_{low}	P_{inter}	*Efficiency	Split Fraction	ΔT PHX	Pre-cooler Mass
	MW/K	-	MPa	MPa	%	-	°C	ton
Recompression	**5**	0.497	8.56	-	47.17	0.87	138.0	53.37
Partial Cooling	**5**	0.564	5.58	10.61	49.99	0.60	180.5	63.30
Recompression	**10**	0.568	10.0	-	50.39	0.73	114.2	48.59
Partial Cooling	**10**	0.454	5.96	10.90	51.21	0.59	170.5	59.23
Recompression	**15**	0.535	10.05	-	51.59	0.70	109.5	46.44
Partial Cooling	**15**	0.375	6.06	10.95	51.49	0.60	168.4	58.43

*Note that the reported thermal efficiency does not include fan parasitics, which are 0.35 MW for each case.

Figure 3 shows a comparison of the recompression and partial cooling cycles on a temperature-entropy diagram for the 15 MW/K conductance case. This plot emphasizes some of the important tabulated data and helps explain how each cycle derives its efficiency. As listed in Table 4 and shown in this figure, the partial cooling cycle optimizes at a higher pressure ratio.
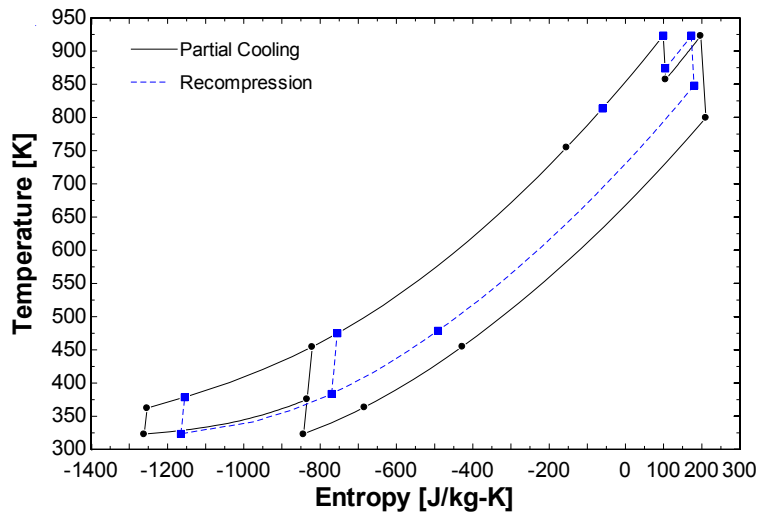

Figure 3: Temperature-entropy diagram of optimized cycles with 15 MW/K recuperator conductance

This feature is afforded to the cycle by the intercooler (intermediate pressure pre-cooler). The higher pressure ratio causes the outlet temperature of the low pressure turbine to be lower than it is in the recompression cycle. In turn, the average heat input temperature is lower for the partial cooling cycle, which all else equal results in lower cycle efficiency. One mitigating effect, however, is that the intercooling stage allows for a lower pressure difference across the main compressor. Consequently, the compressor outlet temperature is lower for the partial cooling cycle, thereby decreasing the high pressure low temperature recuperator outlet temperature and allowing the cycle to reject heat at a lower average temperature. Finally, the higher pressure ratio results in a lower required mass flow rate to generate a given amount of power. Therefore, recuperators in the partial cooling cycle will have a lower duty, and it follows that for a set recuperator conductance the cycle with the lower duty will likely experience greater effectiveness in the recuperators.

4.1. Limitations

Figure 2 suggests that the partial cooling cycle offers an efficiency advantage over the recompression cycle at most quantities of recuperator conductance. The purpose of this study was to compare the selected cycles on an equivalent basis using recuperator conductance and pre-cooler sizing models that can be used as a proxy for the total material used, and therefore, the cost. While these models improve upon the effectiveness model used in previous analyses, they do contain assumptions that likely impact the results:

4.1.1. Recuperator modeling

- The conductance model (along with the entire cycle model) does not consider pressure drops. Therefore, the density of the fluid has no impact on heat exchanger size. For example, a lower density fluid may require a trade-off between more cross-sectional flow area and a higher pressure drop. The low-side stream in the partial cooling cycle will have a lower density than the low-side stream in the recompression cycle.
- The conductance model does not consider the effect of absolute pressures and pressure differentials on the material thicknesses (and therefore conductance) of the heat exchangers. The partial cooling cycle has a larger pressure ratio than the recompression cycle; however, it has a lower absolute pressure.
- The conductance model does not calculate the convective heat transfer coefficients of the fluid, and therefore does not assess possible differences in conductance between cycles due to varying fluid properties.

4.1.2. Pre-cooler modeling

The pre-cooler mass is calculated by first optimizing the cycle model, and then solving the pre-cooler model using the design parameters in Table 2. In reality, the cycle model would be optimized concurrently with the pre-cooler model. For example, the fan power might be increased to limit the total pre-cooler mass, or the compressor inlet temperature or pressure ratio may be adjusted to achieve more favorable cooling conditions at the expense of cycle efficiency. Like the recuperator model, the pre-cooler model does not consider pressure drops or the effect of absolute pressure on material thickness.

5. Cycle integration with CSP systems

5.1. Sensible heat thermal storage

Recent work has highlighted the economic benefit of CSP plants with thermal storage [13], [14]. Sensible heat storage systems have been demonstrated at temperatures around 560°C and are being researched for higher temperatures to meet SunShot objectives. As stated in the introduction, the temperature difference between the inlet and outlet of the primary heat exchanger has a direct impact on the cost of a sensible heat transfer system. Table 4 shows that this temperature difference in the partial cooling cycle is between 23% and 35% larger than in the recompression cycle, depending on the recuperator conductance. This may result in a similar cost savings for sensible heat thermal storage integrated with a partial cooling cycle at SunShot conditions. Furthermore, the partial cooling cycle maintains its larger temperature difference across the primary heat exchanger at current power tower conditions, although the impact of lower temperatures on the cycle efficiency relative to the recompression cycle has not been analyzed.

5.2. Direct CO2 receivers

NREL [15], Brayton Energy [16], Oregon State University [17], and others are currently investigating receivers that use CO2 as the working fluid. One potential implementation of a CO2 receiver is to use the receiver as the primary heat exchanger in the power cycle, thereby directly using the power cycle working fluid as the receiver heat transfer fluid. The characteristics of the partial cooling cycle may also confer some advantages for these receivers.
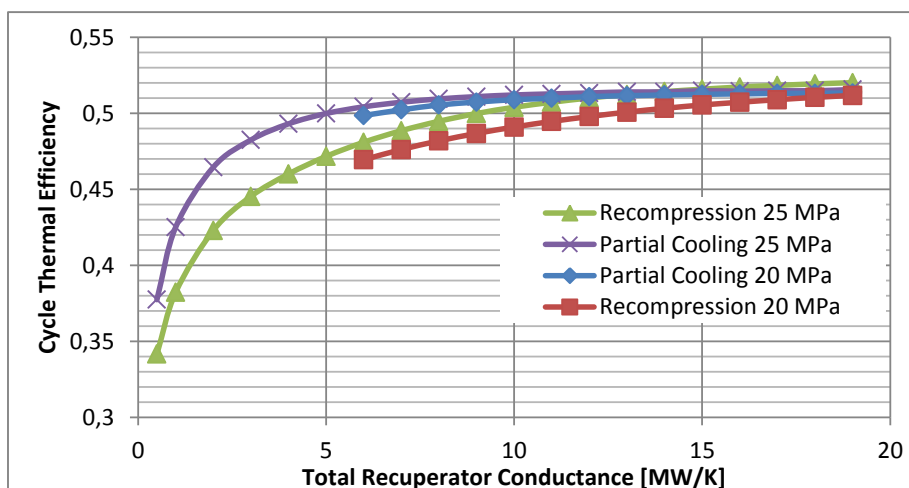
Figure 4: Analysis of optimized cycle thermal efficiency vs. recuperator conductance at 20 and 25 MPa upper pressures.

A CSP receiver will experience at least partial exposure to the environment. Therefore, the receiver incurs thermal emissive and convective losses correlated to the temperature of the receiver. The partial cooling cycle may improve receiver thermal efficiency by lowering the average operating temperature of the receiver.

If a tubular receiver concept is considered and the mass flow rate through the tubes is fairly constant between the partial cooling and recompression receivers, then the partial cooling receiver will have longer flow paths (while the recompression receiver would have a greater number of shorter flow paths in parallel). This feature may help the design of a direct receiver in two ways. 1) Longer flow paths help stabilize the mass flow through parallel tubes connected to the same header. 2) More surface area per flow path will be available that can help reduce the deviation of absorbed energy and maintain similar outlet temperatures across parallel tubes and flow paths. 3) Although both the partial cooling and recompression direct receivers require around the same heat input, the mass flow rate to the receiver is lower for the partial cooling cycle. It follows that designs with significant piping to the receiver may be able to reduce the size of the pipes connecting the receiver to the power block.

Finally, the partial cooling cycle grants greater potential to lower the high pressure in the cycle. Figure 4 shows that at an upper pressure of 20 MPa the partial cooling cycle nearly matches the performance of the design cases at 25 MPa, while the recompression cycle at 20 MPa suffers a significant efficiency penalty until large recuperator conductance values are included. The lower pressure design may be particularly suited for direct receiver applications as the combination of high pressure and high temperature causes the required tube thickness to significantly increase. By decreasing the pressure, the design gains flexibility to decrease thickness, and possibly increase the allowable incident flux or receiver fatigue life. It should be noted that the partial cooling cycle at 20 MPa operates at a lower pressure ratio, which decreases the temperature difference over the primary heat exchanger. The model shows that at 10 MW/K the 20 MPa model has a temperature difference of 161.5°C, while the 25 MPa model has a difference of 170.5°C and the recompression cycle at 20 MPa has a difference of 114.2°C.

6. Conclusions

This study investigates the performance of the simple, recompression, and partial cooling cycles under design-point conditions relevant to CSP. Results showed that when specifying an effectiveness to model the recuperator(s), the performance of the partial cooling and recompression cycles were similar. However, when specifying a conductance to model the recuperator(s), the partial cooling cycle outperformed the recompression cycle until large quantities of conductance were modeled. It is pointed out that while the conductance model is a better proxy for

physical heat exchanger size than the effectiveness model, it still contains simplifications whose impact need to be understood. A key benefit of the partial cooling cycle for CSP applications is a larger temperature differential across the primary heat exchanger, which allows for more cost efficient sensible thermal energy storage systems and possible more thermally efficient receivers as well. The results presented in this paper do not make a definitive case for the partial cooling cycle over the recompression cycle, but it is hoped that the results motivate further detailed studies on the partial cooling cycle similar to those completed on the simple and recompression cycles in order to better understand potential advantages.

Acknowledgements

References

[1] C. S. Turchi, Z. Ma, T. W. Neises, and M. J. Wagner, "Thermodynamic Study of Advanced Supercritical Carbon Dioxide Power Cycles for Concentrating Solar Power Systems," *Journal of Solar Energy Engineering*, vol. 135, no. 4, p. 041007, Jun. 2013.
[2] V. Dostal, M. J. Driscoll, and P. Hejzlar, "Advanced Nuclear Power Technology Program A Supercritical Carbon Dioxide Cycle for Next Generation Nuclear Reactors," MIT, 2004.
[3] V. Dostal and M. Kulhanek, "Research on the Supercritical Carbon Dioxide Cycles in the Czech Republic," in *Proceedings of the 2009 Supercritical CO2 Power Cycle Symposium*, 2009.
[4] W. Seidel, "Model Development and Annual Simulation of the Supercritical Carbon Dioxide Brayton Cycle for Concentrating Solar Power *Applications* by," University of Wisconsin - Madison, 2010.
[5] J. C. *Bryant*, H. Saari, and K. Zanganeh, "An Analysis and Comparison of the Simple and Recompression Supercritical CO2 Cycles," in *Supercritical CO2 Power Cycle Symposium*, 2011.
[6] M. Kulhánek and V. Dostal, "Thermodynamic Analysis and Comparison of Supercritical Carbon Dioxide Cycles," in *Proceedings of the 2011 Supercritical CO2 Power Cycle SymposiumSupercritical CO2 Power Cycle Symposium*, 2011, pp. 2–8.
[7] J. J. Dyreby, S. A. Klein, G. F. Nellis, and D. T. Reindl, "MODELING OFF-DESIGN AND PART-LOAD PERFORMANCE OF SUPERCRITICAL CARBON DIOXIDE POWER CYCLES," in *Proceedings of ASME Turbo Expo 2013*, 2013, pp. 1–7.
[8] J. J. Dyreby, S. A. Klein, G. F. Nellis, and D. T. Reindl, "Development of Advanced Models for Supercritical Carbon Dioxide Power Cycles for Use in Concentrating Solar Power Systems - Subcontract No. AXL-0-40301-1 to National Renewable Energy Laboratory," 2012.
[9] C. S. Turchi, "Supercritical CO 2 for Application in Concentrating Solar Power Systems," in *Proceedings of Supercritical CO2 Power Cycle Symposium*, 2009, no. Figure 1, pp. 1–5.
[10] C. S. Turchi, Z. Ma, T. Neises, and M. Wagner, "Thermodynamic Study of Advanced Supercritical Carbon Dioxide Power Cycles for High Performance Concentrating Solar Power Systems - Preprint," in *Proceedings of ASME 2012 6th International Conference on Energy Sustainability & 9th Fuel Cell Science, Engineering and Technology Conference*, 2012.
[11] D. J. Gavic, "Investigation of Water, Air, and Hybrid Cooling for Supercritical Carbon Dioxide Brayton Cycles," University of Wisconsin-Madison, 2012.
[12] "Klein, S.A. (2010). EES – Engineering Equation Solver, F-Chart Software. http://www.fchart.com.," p. 2010, 2010.
[13] P. Denholm, Y. Wan, M. Hummon, and M. Mehos, "An Analysis of Concentrating Solar Power with Thermal Energy Storage in a California 33 % Renewable Scenario An Analysis of Concentrating Solar Power with Thermal Energy Storage in a California 33 % Renewable Scenario," 2013.
[14] P. Denholm and M. Mehos, "Enabling Greater Penetration of Solar Power via the Use of CSP with Thermal Energy Storage," NREL, Golden, CO, 2011.
[15] U.S. Department of Energy, "SunShot Initiative: Direct Supercritical Carbon Dioxide Receiver Development," 2013. [Online]. Available: http://www1.eere.energy.gov/solar/sunshot/lab_nrel_receiver.html.
[16] U.S. Department of Energy, "SunShot Initiative: High-Efficiency Receivers for Supercritical Carbon Dioxide Cycles," 2013. [Online]. Available: http://www1.eere.energy.gov/solar/sunshot/csp_sunshotrnd_brayton.html.
[17] U.S. Department of Energy, "SunShot Initiative: High-Flux Microchannel Solar Receiver," 2013. [Online]. Available: http://www1.eere.energy.gov/solar/sunshot/csp_sunshotrnd_oregon.html.